European Journal of Radiology 186 (2025) 112033

Contents lists available at ScienceDirect

European Journal of Radiology

journal homepage: www.elsevier.com/locate/ejrad

Fast (< 30 min) "All-in-One" whole-body MRI for TNM staging in high-risk prostate cancer (PCa): Feasibility and comparison to ^{68}Ga-Prostate Specific Membrane Antigen (PSMA)-PET/CT☆

Sandy Van Nieuwenhove [a], Renaud Lhommel [b], Vassiliki Pasoglou [a], Julien Van Damme [c], Nicolas Michoux [a], Perrine Triqueneaux [a], Bertrand Tombal [c], Frédéric E. Lecouvet [a,*]

[a] Institut du Cancer Roi Albert 2 (IRA2) and Institut de Recherche Expérimentale & Clinique (IREC) Department of Radiology (IMAG), Université Catholique de Louvain (UCLouvain) – Cliniques Universitaires Saint Luc, Brussels, Belgium
[b] Institut du Cancer Roi Albert 2 (IRA2) and Institut de Recherche Expérimentale & Clinique (IREC), Department of Nuclear Medicine, Université Catholique de Louvain (UCLouvain) – Cliniques Universitaires Saint Luc, Brussels, Belgium
[c] Institut du Cancer Roi Albert 2 (IRA2) and Institut de Recherche Expérimentale & Clinique (IREC) Department of Urology and Department of Experimental Surgery and Transplantation (CHEX), Université Catholique de Louvain (UCLouvain) – Cliniques Universitaires Saint Luc, Brussels, Belgium

ARTICLE INFO

Keywords:
Magnetic resonance imaging
Whole body imaging
PSMA-PET CT
Prostate cancer
Staging

ABSTRACT

Purpose: Next-generation imaging techniques, including PSMA-PET/CT and whole-body MRI (WB-MRI), are disrupting the management of prostate cancer (PCa). This study aimed to build a fast "All-In-One" WB-MRI protocol and to compare it to ^{68}Ga-PSMA-PET/CT for local (T), nodal (N), and distant staging (M1a, M1b, M1c).
Methods: Fifty-two PCa patients at high-risk for metastases underwent a fast "All-in-One" WB-MRI (combining biparametric prostate assessment based on rapid T2-weighted and diffusion-weighted imaging (DWI) following the PI-RADS v2.1 guidelines and the MET-RADS-P guidelines). This WB-MRI prococol was compared to routinely performed PSMA-PET/CT read according to PSMA-RADS 1.0. Inter-technique agreement on staging and proportion differences in positive findings were assessed using Gwet's AC1 and Exact test.
Results: Fast "All-in-One" WB-MRI better detected local tumors (T) (87 % vs 77 %, $p = 0.063$), while PSMA-PET/CT detected more nodes (40 % vs 29 %, $p = 0.031$) with a median small axis of 5 mm. No proportion difference was observed in the detection of extra nodal metastases (M1b) ($p > 0.999$). Inter-technique agreement ranged from good ($AC1^{M1a} = 0.68$, $AC1^{N} = 0.79$) to very good ($AC1^{T} = 0.86$, $AC1^{EPE} = 0.89$, $AC1^{M1b} = 0.93$, $AC1^{M1c} = 0.96$). Fewer oligometastatic patients were detected with PSMA-PET/CT (11 %) compared to WB-MRI (19 %).
Conclusion: A fast (<30 min) "All-In-One" WB-MRI protocol can be implemented in clinical routine. It provides better anatomical characterization of the T2/T3 stage than ^{68}Ga-PSMA-PET/CT, similar distant metastasis detection rate, but slightly inferior detection rate of nodal metastases.

1. Introduction

The management of prostate cancer (PCa) relies on the optimal staging of newly diagnosed high-risk patients and recurrent disease. Multiparametric prostate magnetic resonance imaging (mp-MRI) is the reference standard for diagnostic and local staging of prostate cancer [1]. Thoraco-abdomino-pelvic computed tomography (TAP-CT) and 99mTc bone scintigraphy (BS) remain the standard diagnostic imaging modalities at diagnosis for high-risk patients [2,3]. The recently published EAU EANM statement recommend ^{68}Ga-PSMA-PET/CT for newly diagnosed high-risk patients, for patients with biochemical recurrence (BCR) who may benefit from local treatment, or to confirm

Abbreviations: ADT, androgen deprivation therapy; BCR, biochemical recurrence; DWI, diffusion weighted-imaging; EPE, Extraprostatic Extension; IQR, Interquartile Range; MET-RADS-P, METastasis Reporting and Data System for Prostate Cancer; mp-MRI, multiparametric MRI; PCa, Prostate cancer; Pi-RADS, Prostate Imaging Reporting and Data System; PSMA-RADS, Prostate-specific Membrane Antigen Reporting and Data System; RP, Radical Prostatectomy; SUV, standardized uptake value; WB-MRI, Whole Body-MRI.

☆ This article is part of a special issue entitled: 'Oncologic Imaging' published in European Journal of Radiology.

* Corresponding author at: Radiology Department, Cliniques Universitaires Saint Luc, Avenue Hippocrate 10, B-1200 Brussels, Belgium.
E-mail address: frederic.lecouvet@saintluc.uclouvain.be (F.E. Lecouvet).

https://doi.org/10.1016/j.ejrad.2025.112033
Received 2 December 2024; Received in revised form 27 February 2025; Accepted 3 March 2025
Available online 13 March 2025

oligometastatic disease before metastasis-directed therapy (MDT) [4,5].

In 2014, Pasoglou and colleagues demonstrated the feasibility of a "one-step TNM staging" of high-risk newly diagnosed PCa patients, combining mp-MRI of the prostate including triplanar T2 fast spin echo (FSE), axial diffusion-weighted imaging (DWI) and dynamic contrast-enhanced MRI, and WB-MRI consisting of coronal 3D T1 and axial DWI of the body and sagittal fat-suppressed proton density images of the spine [6]. In 2017, Robertson and colleagues showed the feasibility of a similar "All-in-One" approach in recurrent PCa [7]. The acquisition time was almost one hour in both studies, which limited their implementation in clinical routine and patient acceptance. Since then, technical advances in WB-MRI, such as the use of breath-hold 3D T1 gradient echo Dixon sequences instead of 3D T1 FSE sequences allowed a 10-fold reduction in acquisition time with even higher image quality [8,9]. Regarding local staging, the introduction of the Pi-RADS v.2 score in 2015 minimized the importance of dynamic contrast-enhanced MRI sequences [10]. Several articles and meta-analyses have shown that a biparametric examination (based on T2-weighted FSE and axial DWI sequences) has pooled specificity and sensitivity similar to that of mp-MRI (including post-contrast sequences) [11–14]. This biparametric approach significantly reduces imaging time for local staging without compromising diagnostic performance [15].

PSMA-PET/CT has been recommended during BCR and in high-risk localized or locally advanced newly diagnosed PCa, to optimize both local and distant staging [16]. Recently, some studies have compared PSMA-PET/CT with mp-MRI for local staging, for the assessment of extraprostatic extension (EPE) and for seminal vesicle invasion, showing comparable sensitivities recently confirmed by a meta-analysis [17].

This study evaluates the feasibility of a fast "All-In-One" WB-MRI protocol and compares its findings to those from daily routine clinical ^{68}Ga-PSMA-PET/CT exams performed to rule out extra-prostatic disease (N, M) in case of high-risk PCa or to identify the site of the BCR.

2. Material and Methods

2.1. Study population

This single-center prospective study included 52 consecutive patients between April 2020 and January 2023 with either newly diagnosed high-risk PCa (38/52) or BCR (14/52) who had routine PSMA-PET/CT in their diagnostic imaging pathway. Inclusion criteria for freshly diagnosed high-risk PCa were defined as PSA levels >20 mg/ml or ISUP (International Society of Urological Pathology) grade ≥4/5 or cT3 or cT4 based on digital rectal examination according to EAU guidelines. Inclusion for BCR was defined as PSA doubling time (PSADT) ≤ 1 year after radical prostatectomy (RP) or pathological Gleason score 8–10 at RP and interval to BCR ≤ 18 months for patients treated with external beam radiotherapy (EBRT) or brachytherapy or pathological Gleason score 8–10 on biopsies. Exclusion criteria were severe claustrophobia and MRI-incompatible implanted medical devices. After institutional review board approval (2019/06FEV/060), written informed consent was obtained from all participants. All patients underwent WB-MRI and PSMA-PET/CT within one month (median 11 days; IQR 7–21 days). Follow-up of the PCa patients was done according to best urological practice including clinical visit and PSA testing for 18 patients and imaging tests upon request based on the appearance of symptoms, suspicion of complications or recurrence.

2.2. MR imaging

The following strategy was adopted to develop a fast "All-in-One" MRI protocol and to reduce the total acquisition time. The examinations were performed on a 1.5 T magnet using a 16-channel phased array coil (1.5 T MR450W GEM, GE HealthCare). For local staging, a biparametric prostate MR protocol was implemented including axial T2-weighted FSE images, coronal and sagittal T2 PROPELLER images and axial DWI images. Recent technical advances in DWI, clinically validated for PCa detection [18], allowed the acquisition of only two b-values b = 50 s/mm^2 and b = 800 s/mm^2 and the calculation of higher b-values images (b = 1400 s/mm^2 and b = 2000 s/mm^2) to reconstruct the apparent diffusion coefficient (ADC) map, thus reducing the acquisition time to 3 min 12 s (compared to a previous biparametric acquisition time of 3 min 55 s) [15]. A low b-value = 50 s/mm^2 was chosen to reduce the contribution of the microperfusion fraction to the ADC following current guidelines [16,19]. Axial FSE images (slice thickness 3 mm) were acquired with a higher number of signal averages to increase the signal-to-noise ratio (6 min 51 s) and to avoid some contrast inconsistencies with the PROPELLER sequences [20].

For locoregional and distant metastatic assessment, a WB-MRI protocol covering the body from head to mid-thigh was performed including breath-hold coronal T1 gradient echo images (LAVA-Flex; 19 s per stack; 3 stacks) and axial WB-DWI (3 min 6 s per stack; 5 stacks). The total acquisition time was 16 min 45 s. Acquisition of 3D T1 images allowed image reconstruction in different planes, and the low b-value DWI image provided T2 equivalent images, allowing the examination to meet MET-RADS-P guidelines [21]. The total acquisition time for the fast "All-In-One" WB-MRI for TNM staging was 29 min 23 s. The acquisition parameters are summarized in Table 1.

2.3. PSMA-PET/CT imaging

The ^{68}Ga-PSMA-PET/CT scan was performed under routine clinical conditions after intravenous injection of a target activity of 111 MBq (IQR 93.6–148 MBq) of locally synthesized ^{68}Ga-PSMA-11 using a Scintomics GRP4V synthesizer (PSMA-HBED-11 labeling kits provided by ABX, Germany; ^{68}Ge/^{68}Ga Galli Ad generator, IRE Elite, Fleurus, Belgium). Images were acquired at least 60 min after injection (IQR 76–88 min) from skull to mid-thigh, on either a Gemini-TF 64-slice or a Vereos digital PET/CT (Philips Healthcare, Best, The Netherlands) and reconstructed with full physical corrections, including attenuation correction based on low-dose CT. For 69 % of the patients, a second abdomino-pelvic contrast-enhanced acquisition was acquired in portal phase (70 s post injection) to improve the visualization of the anatomical background and lymph nodes discrimination from the surrounding structures (vessels, ureteral tracts, gut…). As routine mp-MRI evaluation was evaluable for each patient, no dedicated PSMA-PET/CT protocol was used to prospectively address the characterization of the extraprostatic PCa extension (no prospective T-stage evaluation). Historical cases were retrieved and anonymized before the blinded revision for the aim of this retrospective comparison with WB-MRI.

2.4. Image reading

All images were reviewed on the institutional picture archiving and communication system (PACS) (Carestream Vue, Philips, Best, The Netherlands) using the workstation's windowing, multiplanar reformation, linking and scrolling tools. Two board-certified radiologists (R1: 3 years' experience, R2: 10 years' experience) performed the MRI readings independently, then reviewed discordances in consensus (being blinded to patient clinical and other imaging information). A board-certified nuclear medicine physician (R3: 20 years of experience) performed the PSMA-PET/CT readings using Osirix MD software (Pixmeo SARL, Bernex, Switzerland). Readings were blinded to other imaging and clinical records. Structured reporting was performed according to PSMA-RADS 1.0 [22].

All readers assessed local tumor extension (T) or recurrence in the prostatic bed according to the PSMA-RADS guidelines for PSMA-PET/CT and Pi-RADS v2.1 for biparametric prostate MR protocol, using the segmentation of each prostate lobe into three parts (base, mid-region and apex) according to PSMA-RADS 1.0. The presence of extraprostatic extension (EPE) on MRI and its localization (extracapsular, seminal vesicle or other) were assessed using the grading system from

Table 1
MRI acquisition parameters. FOV, Field of View; TR, Repetition Time; TE, Echo Time; DWI, diffusion weighted-imaging; EPI-SPAIR, Spectral Attenuated Inversion Recovery; LAVA-Flex, liver imaging with volume acceleration-flexible; NEX, number of Excitations; TA, Time of acquisition.

Sequence type	Prostate bed assessment				Whole-Body assessment	
	T2 FSE	T2 PROPELLER	T2 PROPELLER	TSE-DWI	LAVA Flex	EPI-SPAIR-DWI
Plane of acquisition	Axial	Sagittal	Coronal	Axial	Coronal	Axial
FOV (mm)	200 × 200	260 × 260	260 × 260	400 × 400	480 × 480	440 × 440
Voxel size (mm)	0.6 × 0.6 × 3.0	0.8 × 0.8 × 3.5	0.8 × 0.8 × 3.5	3.1 × 3.1 × 4.0	1.5 × 1.5 × 4.0	4.6 × 3.4 × 6.0
TR/TE (ms)	8388/100	5576/100	5576/100	5200/72.9	6.1/2.1	10,235/72.1
Flip angle (°)	–	–	–	–	12	–
NEX	3	1.5	1.5		0.5	–
***b*-value**	–	–	–	b = 50 s/mm^2 and b = 800 s/mm^2 Calculated b = 1400 s/mm^2 b = 2000 s/mm^2	–	b = 50 s/mm^2 and b = 800 s/mm^2
Breathing management	Free breathing	Free breathing	Free breathing	Free breathing	Breath-hold	Respiratory gating for chest and abdominal stacks
TA per stack (min, s)	6 min 51 s	1 min 13 s	1 min 07 s	3 min 12 s	0.19 s	3 min 06 s
Number of stacks	1	1	1	1	3	5
Total TA (min,s)	6 min 51s	1 min 13 s	1 min 07 s	3 min 12 s	57 s	15 min 30 s

Mehralivand et al [23]. Tumor Contact Length (TCL) was also measured for each lesion. Evaluation of EPE on clinical PSMA-PET/CT was visually assessed as positive according to maximum standardized uptake values (SUV max) outside the prostatic gland or at the level of the seminal vesicle as previously described [24].

Locoregional lymph nodes were considered pathological at MRI if their short axis was > 8 mm in the pelvic region, > 5 mm in the mesorectum (pararectal), and ≥ 10 mm in the retroperitoneal space. At PSMA-PET/CT, they were considered pathological if there was intense uptake of lymph nodes (SUVmax > 3) regardless of their small axis (PSMA-RADS 4) or lymph nodes with intense uptake and a short axis >10 mm (PSMA-RADS 5) [25]. Locoregional nodes (N) were categorized into five anatomical regions: internal iliac, external iliac, obturator, presacral and other pelvic regions. Distant metastatic nodes (M1a) were classified into four regions: common iliac, retroperitoneal and supradiaphragmatic.

Bone metastases (M1b) were considered pathological on WB-MRI according to the MET-RADS-P guidelines if showing low signal intensity on T1 and high signal on DWI images, with a diameter ≥10 mm [21]. Six anatomical regions were considered: pelvis, lumbar spine, dorsal spine, cervical spine, thorax including sternum, scapula and ribs, and appendicular including both femurs and humerus. Other metastatic sites (M1c) included liver, lung and adrenal glands. On PSMA-PET/CT, metastatic sites were considered pathological if there was intense uptake, superior to the surrounding background (and SUVmax > 3).

For each stage (T, N, M1a, M1b, M1c), a categorical score (presence of at least one lesion = yes/no corresponding to a score = 1/0) was assessed. For local staging (T), numerical scores (T0, T1-2, T3a-b and T4) were reported. The presence/absence of EPE, their grade on MRI (T3a-b and T4 together) was also assessed. The number of bone metastases (M1b) was assessed using a semi-quantitative score coded on the following scale: no lesion = score 0, 1 lesion = score 1; 2–4 lesions = score 2; 5–10 lesions = score 3; and > 10 lesions = score 4.

2.5. Statistical analysis

Summary characteristics of the patient population were reported as mean values (median values when the data distributions were non-normal according to the Shapiro-Wilk test) and as proportions, with their associated 95 % Confidence Interval (CI) given into brackets.

Inter-technique agreement on staging (T, N, M1a, M1b and M1c) and on the semi-quantitative count of bone metastases (M1b) were assessed using Gwet's AC1 agreement coefficient [26]. Strength of agreement was interpreted as follows: poor: AC1 < 0.20, fair: 0.20 ≤ AC1 < 0.40, moderate: 0.40 ≤ AC1 < 0.60, good: 0.60 ≤ AC1 < 0.80, very good: AC1 ≤ 0.80.

A 2-sided paired Exact test was used to assess proportion differences between MRI and PSMA-PET/CT in terms of positive findings in T, N, M1a, M1b and M1c. The distribution of differences between MRI and PSMA-PET/CT regarding the semi-quantitative count of bone metastases (M1b) was also examined.

Statistical significance was declared at a *p*-value < 0.05 for all the above tests. All calculations were performed using Statsdirect software v3.3.5.

3. Results

3.1. Population

Of the 58 patients eligible for inclusion, 6 were excluded due to incomplete, missing or poor quality PSMA-PET imaging data (Fig. 1). Of the 52 patients included, 38 patients presented with newly diagnosed PCa and 14 patients presented with BCR after RP (3/14), ADT (1/14),

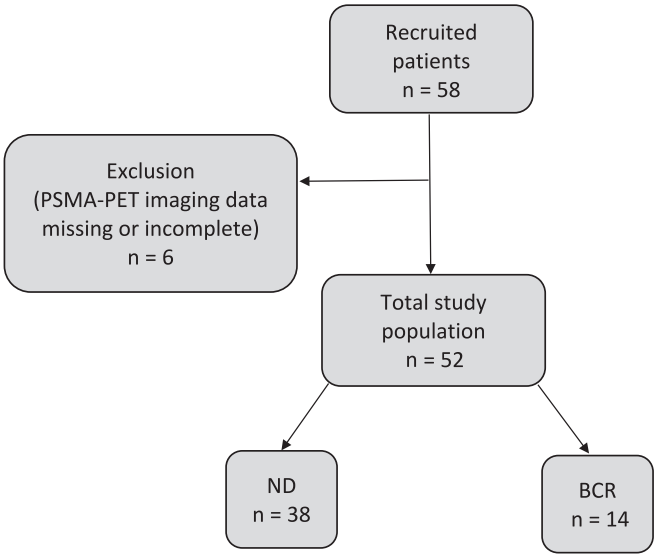

Fig. 1. Study flow chart. ND = newly diagnosed; BCR = biochemical recurrence.

radiotherapy (7/14), brachytherapy (3/14). Patient demographics are shown in Table 2.

3.2. Staging

Staging according to each imaging technique ("All-in-One" WB-MRI and PSMA-PET/CT) is shown in Table 3. A total of 40/52 patients were positive for a local lesion (T) according to both techniques (Fig. 2), while 7/52 patients were negative according to both techniques. T staging results according to fast WB-MRI and PSMA-PET/CT are included in Table 3. A slightly higher TCL measure was observed with PSMA-PET/CT compared to MRI (difference = +3.75 mm [+0.50 mm; +7.50 mm], $p = 0.016$). MRI detected intra-prostatic PCa without any significant PSMA expression in 5/52 patients (proportion difference = +10 %, $p = 0.063$) (Fig. 3) (Table 4).

Twenty-one and fifteen patients had locoregional pathological lymph nodes, according to PSMA-PET/CT and to WB-MRI, respectively (proportion difference = +12 %, $p = 0.031$). There was concordance in N staging in 15 patients (Fig. 4). PSMA-PET/CT detected 6 additional patients with pathological loco-regional lymph nodes (Fig. 5) -and 4 additional patients with pathological distant metastatic lymph nodes in patients with both lymph node and bone metastases. This resulted in more patients with localized PCa on the "All-in-One" WB-MRI (34 vs 30 patients).

Both imaging techniques detected only three patients with distant metastatic lymph nodes (M1a), whereas PSMA-PET/CT detected four more M1a lesions in patients with M1b disease. Both imaging techniques detected 19 patients with bone metastases and 2 patients with both visceral and bone metastases (Fig. 6).

3.3. Inter-technique agreement

AC1 agreement coefficients are shown in Table 4. Inter-technique agreement on the presence or absence (in case of BCR) of PCa in the prostatic bed was very good ($AC1^{T} = 0.86$). Agreement on the value of the local staging was good ($AC1^{numerical\ T} = 0.75$) (Fig. 2). Five T0 patients according to PSMA-PET/CT were assessed as T1-2 (n = 1), T3a-b (n = 3) and T4 (n = 1) by WB-MRI confirmed by histopathological results (Fig. 3). Two T1-2 patients according to PSMA-PET/CT were assessed as T3a-b (n = 1) (Fig. 7) and T4 (n = 1) by WB-MRI. Two T3a-b patients according to PSMA-PET/CT were assessed as T1-2 by WB-MRI. One T4 patient according to PSMA-PET/CT was assessed as T3a-b by WB-MRI.

In the subgroup of patients with local staging (T) > T0, the inter-technique agreement for suspicion of EPE was very good ($AC1^{EPE} = 0.83$). According to both techniques, 27/40 patients had an EPE and 9/40 had not. Two patients had EPE according to either WB-MRI only or PSMA-PET/CT only. There were discrepancies between the two techniques for T3a/T3b/T4 stage assessment in 4 patients, as these stages are better characterized by MRI due to the lack of clear anatomical delineation of the sphincters (external/vesical), feet of seminal vesicles, and topography of capsule boundaries on PSMA-PET/CT (Fig. 7).

Inter-technique agreement on N and M1a stages was good ($AC1^{N} = 0.79$, $AC1^{M1a} = 0.68$) while it was very good for M1b and M1c stages ($AC1^{M1b} = 0.93$, $AC1^{M1c} = 0.96$). The proportion of positive findings detected by one imaging technique but not the other was in N (0.0 % in MRI only; 12 % in PSMA-PET/CT only), in M1a (7.7 % in MRI only; 13 % in PSMA-PET/CT only), in M1b (1.9 % in MRI only, 1.9 % in PSMA-PET/CT only) and in M1c (1.9 % in MRI only, 1.9 % in PSMA-PET/CT only).

Inter-technique agreement on the semi-quantitative count of bone metastases (M1b) was very good ($AC1^{M1b} = 0.87$). The distribution of differences in the semi-quantitative score showed the following trends. Differences in score were at worst equal to 1. A higher score corresponding to a higher number of lesions was observed in 1.9 % (1/52 patients) with MRI (compared to PSMA-PET/CT) and in 9.6 % (5/52 patients) with PSMA-PET/CT (compared to MRI). PSMA-PET/CT detected 9.6 % of lesions smaller than 5 mm (Fig. 8), while WB-MRI only detected bone lesions of at least 10 mm [21]. Fewer oligometastatic patients were detected with PSMA-PET/CT (11 %, 6/52) compared to MRI (19 %, 10/52).

Table 2
Patient characteristics. ND, newly diagnosed; BCR, biochemical recurrence; EBRT, external beam radiation therapy; PSA DT, PSA doubling time; RP, radical prostatectomy; ISUP, International Society of Urological Pathology; ADT, androgen deprivation therapy, ARTA: androgen receptor targeted-agents.

Patient characteristics	ND (n = 38)	BCR (n = 14)
Age, median (IQR), years	71.4 (61.6–73.4)	71.8 (64.1—85.3)
PSA, mean (IQR), ng/ml	11.7 (7.30–40.8)	11.5 (6.40–23.7)
PSA density (IQR), ng/ml	0.35 (0.18–1.03)	0.28 (0.16–0.69)
PSADT, mean (IQR), years	0.40 (0.25–0.70)	0.47 (0.30–0.70)
Clinical stage		
cT1	0	2
cT2	7	6
cT3	22	5
cT4	5	1
ISUP grade		
1	0	2
2	0	3
3	4	2
4	8	2
5	22	5
Treatment	**Treatment post-diagnosis**	**Previous treatment**
ADT	10	1
RP	8	3
EBRT + ADT	8	7
Brachytherapy	0	3
ADT + chemotherapy	3	0
ADT + ARTA	5	0

Table 3
Patient staging with WB-MRI and with PSMA-PET/CT. csPCa, clinically significant PCa; EPE, Extraprostatic Extension; N1, unilateral regional nodes; N2, bilateral regional nodes; M1a; distant nodes; M1b, bone metastasis; M1c, extraosseous/visceral metastasis; T, tumor

Patient staging	Fast "All-in-One" WB-MRI	^{68}Ga-PSMA-PET/CT
Local staging		
T	87 % (45/52)	77 % (40/52)
Tumor Contact Length (TCL)*	30 mm [20 mm; 36 mm]	35 mm [24 mm; 42 mm]
T0	13 % (7/52)	23 % (12/52)
T1-T2	25 % (13/52)	21 % (11/52)
T3a-b	54 % (28/52)	48 % (25/52)
T4	9.6 % (5/52)	7.7 % (4/52)
EPE (T3a-b + T4)	64 % (33/52)	56 % (29/52)
EPE grade 1	9.0 % (3/34)	–
EPE grade 2	50 % (17/34)	–
EPE grade 3	41 % (14/34)	–
Nodes		
N1	21 % (11/52)	25 % (13/52)
N2	7.7 % (4/52)	15 % (8/52)
Distant metastases		
M1a	5.7 % (3/52)	5.7 (3/52)
M1b	36 % (19/52)	36 % (19/52)
M1a within M1b	13 % (7/52)	21 % (11/52)
M1c	3.9 % (2/52)	3.9 % (2/52)
Localized csPCa	65 % (34/52)	57 % (30/52)
Oligometastatic (n ≤ 4)	19 % (10/52)	11 % (6/52)

* A slightly higher TCL measure was observed with PSMA-PET/CT compared to MRI (difference = +3.75 mm [+0.50 mm; +7.50 mm], $p = 0.016$).

4. Discussion

The "All-in-One" WB-MRI approach to PCa combines local cancer assessment with distant node and metastasis screening in a single imaging step. In newly diagnosed PCa with a high risk of metastasis/locally advanced disease, both local and distant staging are required before

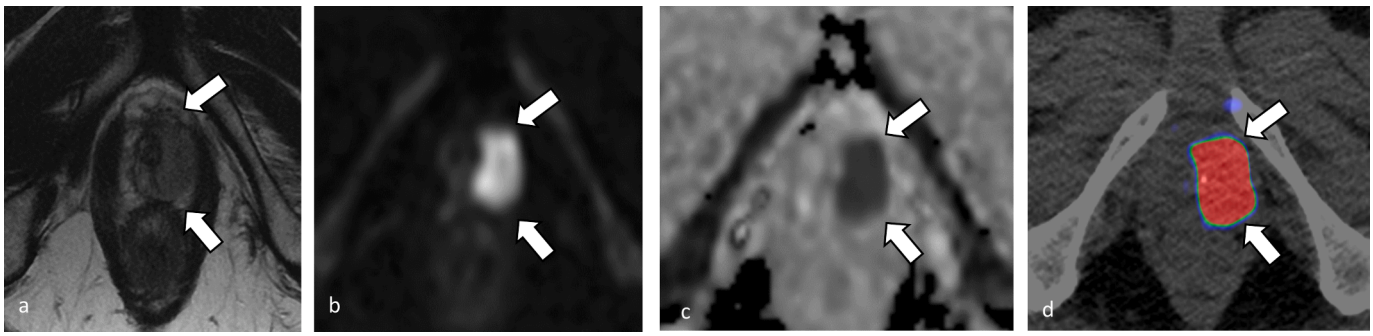

Fig. 2. Concordant local extension according to both the fast "All-in-One" WB-MRI and the ^{68}Ga-PSMA-PET/CT, in a 65-year-old man with a PSA = 8.2 ng/ml who had benefited from radical prostatectomy. Panels a-c (fast "All-in-One" WB-MRI) showed a Pi-RADS 5 lesion of 18 mm confined in the left posterolateral, posteromedian and anterior apex (arrows) with low signal intensity on T2-weighted images (a), restriction of diffusion on high b-value (b = 2000 s/mm^2) (b), and an ADC = 0.52 × 10^3 mm^2/s (c). Transverse section of fused ^{68}Ga-PSMA-PET/CT image showed the same localized lesion (d). Absence of EPE was confirmed on the prostatectomy specimen (pT2c).

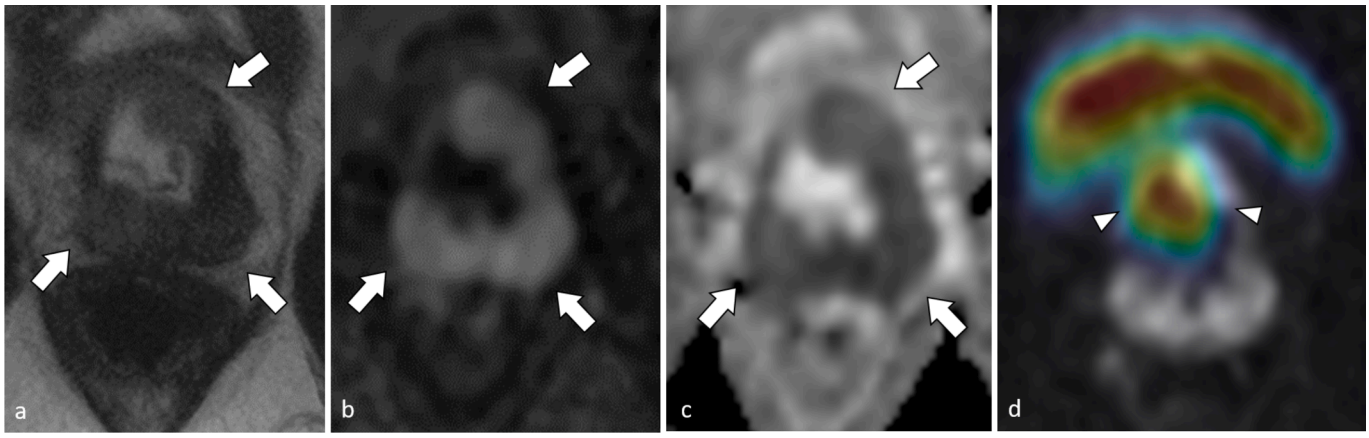

Fig. 3. Discrepancy in local staging between fast "All-in-One" WB-MRI and ^{68}Ga-PSMA-PET/CT, in a 72-year-old man with a PSA = 4.6 ng/ml with TURP and diffuse ISUP 5 at histopathology. Panels a-c (fast "All-in-One" WB-MRI) showed a Pi-RADS 5 lesion infiltrating both lobes (arrows) with low signal intensity on axial T2-weighted images (a), restricted diffusion on high b-value (b = 2000 s/mm^2) (b), and an ADC = 0.62 × 10^3 mm^2/s (c). Panel (d) (transverse section of the fused ^{68}Ga-PSMA-PET and axial DWI image (b = 2000 s/mm^2) were obtained for comparison) showed only excreted urinary activity at the site of TURP cavity (arrowheads), without any ^{68}Ga-PSMA uptake of the pathological infiltrating prostate cancer (d).

Table 4
Inter-technique agreement on positive findings and on extracapsular extension. A 2-sided Exact test (at $p < 0.05$) is used to assess the significance of proportion differences. T, tumor; exact T, T0, T1-2, T3a-b, T4; N, node; M1a, distant node; M1b, bone metastasis; M1c, extraosseous/visceral metastasis; EPE, extraprostatic extension.

	WB-MRI	PET	Proportion difference	Agreement	Discordances		
	positive findings	positive findings		AC1	MRI + only	PET + only	Total
Prostatic lesion	87 % (45/52)	77 % (40/52)	+10 % [+0.5 %; +20 %] for WB-MRI $p = 0.063$	0.86 [0.74; 0.99]	9.6 % (5/52)	0.0 % (0/52)	9.6 % (5/52)
T	–	–	–	0.75 [0.62; 0.89]	–	–	–
N	29 % (15/52)	40 % (21/52)	+12 % [+2.1 %; +21 %] for PET $p = 0.031$	0.79 [0.62; 0.95]	0.0 % (0/52)	12 % (6/52)	12 % (6/52)
M1a	19 % (10/52)	25 % (13/52)	$p = 0.549$	0.68 [0.48; 0.87]	7.7 % (4/52)	13 % (7/52)	21 % (11/52)
M1b	37 % (19/52)	37 % (19/52)	$p > 0.999$	0.93 [0.83; 1.03]	1.9 % (1/52)	1.9 % (1/52)	3.9 % (2/52)
M1c	3.9 % (2/52)	3.9 % (2/52)	$p > 0.999$	0.96 [0.90; 1.02]	1.9 % (1/52)	1.9 % (1/52)	3.9 % (2/52)
Subgroup of patients with staging T > T0 according to both techniques							
EPE (T3a-b + T4)	73 % (29/40)	73 % (29/40)	$p > 0.999$	0.83 [0.67; 1.00]	5.0 % (2/40)	5.0 % (2/40)	10 % (4/40)

treatment decision. At BCR, evidence and localization help tailor salvage treatments, as the disease may involve the prostate bed, lymph node or other metastatic area. Providing local and distant staging in a single imaging session allows a straightforward and comprehensive diagnosis. It shortens the diagnostic pathway and reduces radiation exposure associated with older generation bone scintigraphy and CT [27]. While PSMA-PET/CT could be preferred when considering surgery in high-risk patients, "All-in-One" WB-MRI is a credible imaging option when the

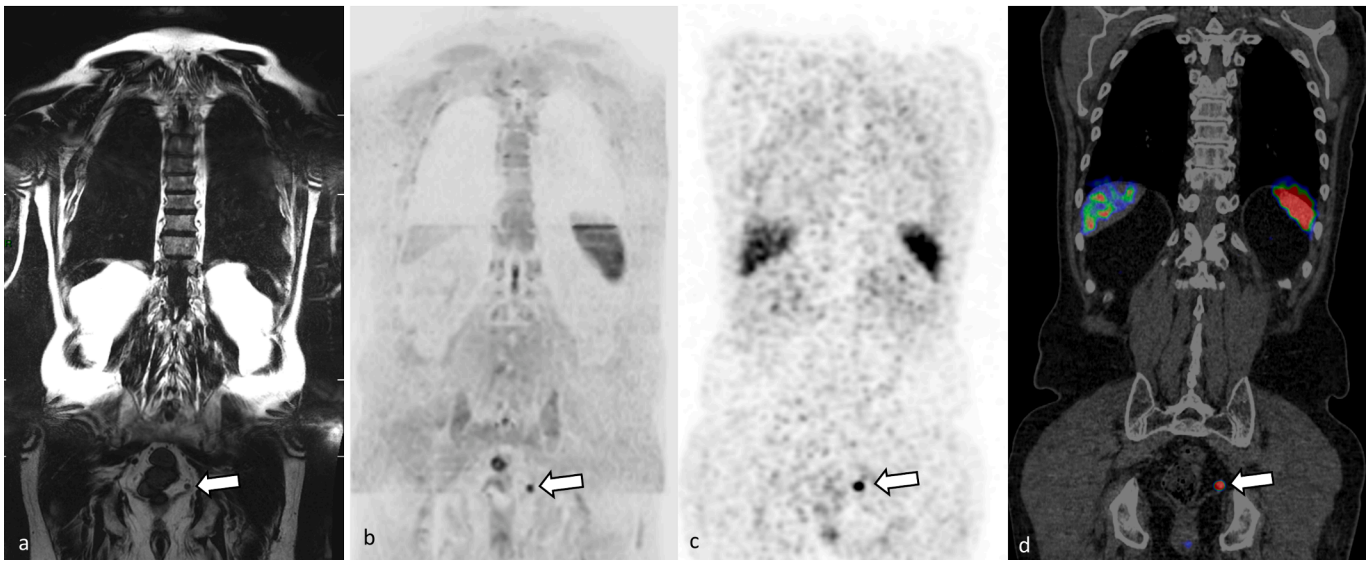

Fig. 4. Concordant lymph node staging between fast "All-in-One" WB-MRI and ^{68}Ga-PSMA PET/CT, in a 75-year-old man with high-risk PCa. Panels a-b (fast "All-in-One" WB-MRI) show coronal WB-MRI T1 Dixon fat only (a), and coronal reformatted DWIBS (b = 1000 s/mm^2; inverted grey scale) images showed a left 8 mm mesorectal lymph node metastasis (arrow) (b). Panels c-d (^{68}Ga-PSMA-PET/CT) show coronal metabolic PET (c), and coronal reformatted fused PET/CT images showed the same lymph node metastasis with PSMA expression (arrow) (d).

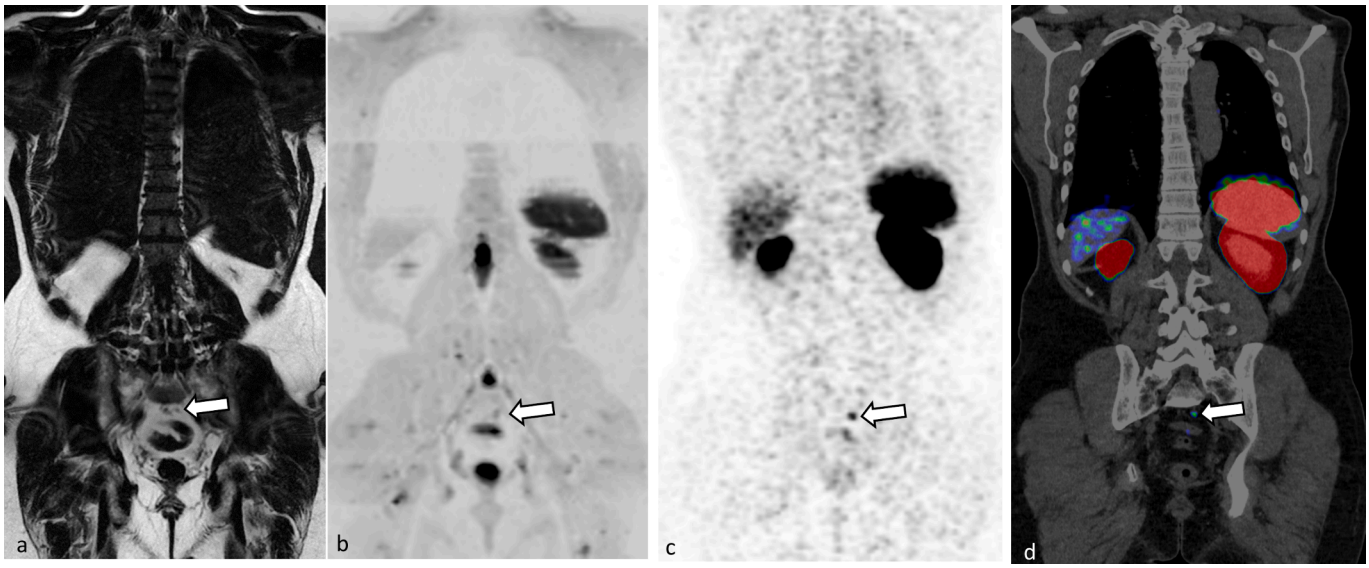

Fig. 5. Discrepancy in lymph node staging between fast "All-in-One" WB-MRI and ^{68}Ga-PSMA-PET/CT, in a 58-year-old man with high-risk PCa. Panels a-b (fast "All-in-One" WB-MRI) show coronal WB-MRI T1 Dixon Fat only (a), and coronal reformatted DWIBS (b = 1000 s/mm^2; inverted grey scale) images showed a retrospective left 4 mm presacral lymph node that was not considered metastatic due to its small size (arrow) (b). Panels c-d (^{68}Ga-PSMA-PET/CT) show coronal metabolic PET (c), and coronal reformatted fused PET/CT with a presacral lymph node metastasis with PSMA expression (arrow) (d).

therapeutic approach consists of systemic treatment +/- local/regional irradiation. MRI can also be used when access to PSMA-PET/CT is limited or associated with long waiting times.

PSMA-PET/CT and WB-MRI are the current optimal approaches for staging PCa [28,29]. Mp-MRI is the gold standard for local assessment of PCa [3]. Previous work has demonstrated the feasibility of combining local and distant staging of PCa in a single MRI session [6,7]. However, despite reducing the number of examinations and appointments, this "All-In-One" approach has not been widely adopted in routine practice due to the long examination duration. Since then, technical advances and careful selection of sequences have significantly reduced the acquisition time. Biparametric prostate MRI allows staging in high-risk patients without compromising performance [30]. Implementing the 3D Dixon gradient echo technique in breath-hold acquisition within a WB-MRI examination is a validated alternative to T1 FSE sequences for detecting skeletal and nodal lesions [21]. It significantly reduces acquisition time. Here, we combined these two approaches in a single MRI session.

The first aim of our study was to build a fast "All-in-One" WB-MRI protocol that could be implemented into daily practice. Our protocol has a total acquisition time of 29 min 23 s, which is acceptable for the patient and imaging professionals. Reducing the duration of MRI examinations by a factor of >2 would allow a greater number of patients to benefit from this technology, reduce the discomfort associated with the examination, and make the process more manageable within MRI units whose schedules are often densely packed with examinations.

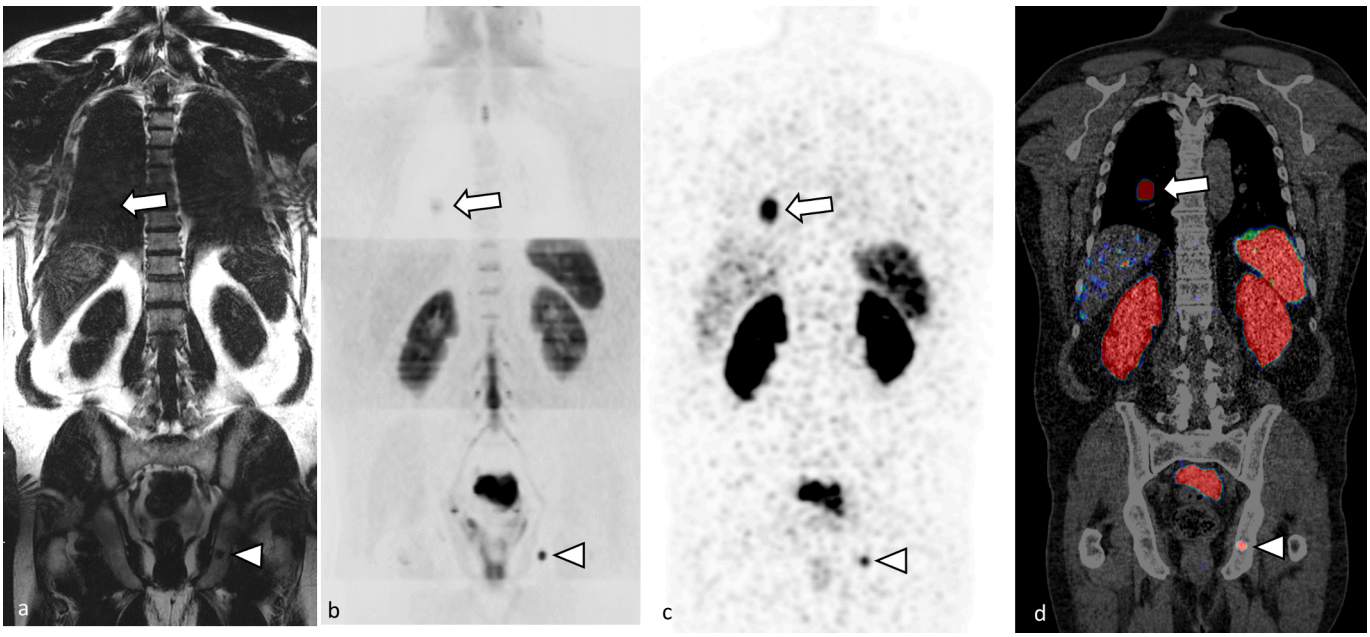

Fig. 6. Concordant evaluation of distant extension between fast "All-in-One" WB-MRI and ^{68}Ga-PSMA-PET/CT in a 63-year-old man with high-risk PCa. Panels a-b (fast "All-in-One" WB-MRI) show coronal WB-MRI T1 Dixon Fat only (a), and coronal reformatted DWIBS (b = 1000 s/mm^2; inverted grey scale) images showed right lung (arrow) and left ischiopubic bone (arrowhead) metastasis (arrow) (b). Panels c-d (^{68}Ga-PSMA-PET/CT) show coronal metabolic PET (c), and coronal reformatted fused PET/CT with the same lung (arrow) and bone metastasis with PSMA expression (arrowhead) (d).

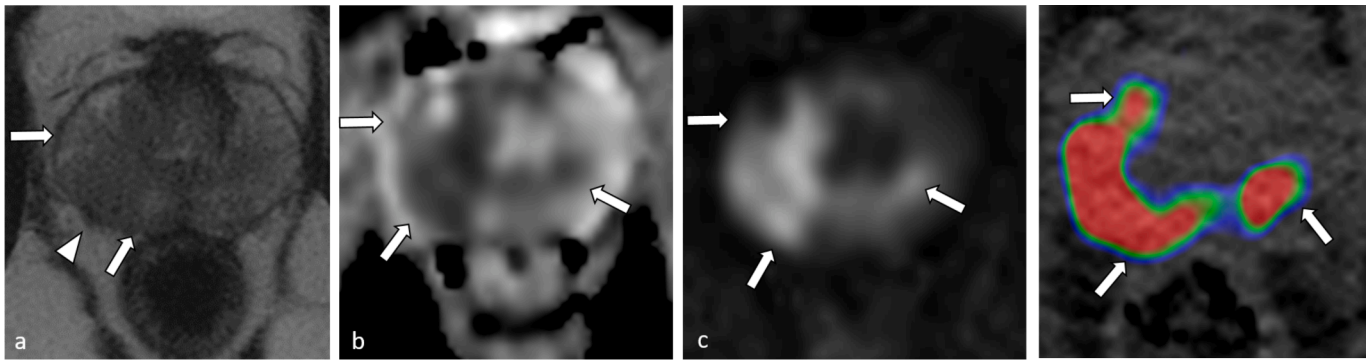

Fig. 7. Discordant local extension between fast "All-in-One" WB-MRI and ^{68}Ga-PSMA-PET/CT, in a 49 year-old man with a PSA = 32.6 ng/ml who benefited from a RP. Biparametric MRI based on on axial T2-weighted images (a), and axial DWI (b = 2000 s/ mm^2) with an ADC map (c) showed a large Pi-RADS 5 lesion infiltrating the right and left lobes (arrows), with low Signal Intensity on T2, restricted diffusion and right posterolateral EPE (arrowhead; EPE2; TCL 41 mm) confirmed pT3a at RP (c). The corresponding transverse section of fused ^{68}Ga-PSMA-PET/CT was not able to detect EPE (d).

The second aim was to compare the diagnostic value of this non-irradiating fast MRI protocol to that of ^{68}Ga-PSMA-PET/CT, the current gold standard for distant staging. Aside from its diagnostic value for whole-body staging, ^{68}Ga-PSMA-PET/CT has also emerged as a valuable strategy for local staging [31]. Of note, one study also suggested a "All-In-One" whole body staging using ^{68}Ga-PSMA-11PET/MRI in high-risk PCa patients [32].

Regarding local assessment, a very good agreement was observed between both techniques, with however a better detection of the primary cancer by the fast WB-MRI (+10 %, $p = 0.063$). These observations are consistent with a systematic review comparing PSMA/PET-CT and mp-MRI for the detection of clinically significant PCa [33]. MRI detected local cancer in five additional patients. Among them, three patients had previously undergone transurethral resection of the prostate (TURP), which may have masked prostate lesions due to the presence urine with high concentration of ^{68}Ga-PSMA [34]. The two other patients showed no ^{68}Ga-PSMA uptake despite confirmation of clinically significant PCa on histology specimen. This observation is consistent with the study by Arslan A et al, who demonstrated superior detection of index lesions on MRI compared to ^{68}Ga-PSMA-/PET/CT [35].

Regarding local extension assessment, MRI tended to detect more EPE compared to PSMA-PET/CT (64 % vs 56 %). The sensitivity of PSMA-PET/CT to detect seminal vesicles infiltration has been reported to be only 75 % when compared with the results of pathological analysis after radical prostatectomy [36]. Our results demonstrating superior assessment of EPE with MRI are in line with a previous study showing a performance in terms of Area Under the ROC curve (using pathological results as reference) of AUC = 0.80 compared to AUC = 0.57 for PSMA-PET/CT [24]. The lower ability of PSMA-PET/CT to characterize PCa invasion at the borders of the prostate may be due to high levels of activity in the urine near the vesico-urethral junction or in the center of the prostate after TURP, leading to false-negative results. It is also related to the lower spatial resolution of PET/CT compared to MRI to correctly localize the critical anatomical boundaries of the gland (feet of the seminal vesicles, prostate capsule, external sphincter, rectal wall) required for a correct T3a-b/T4 staging [34]. Studies using 18-F PSMA-

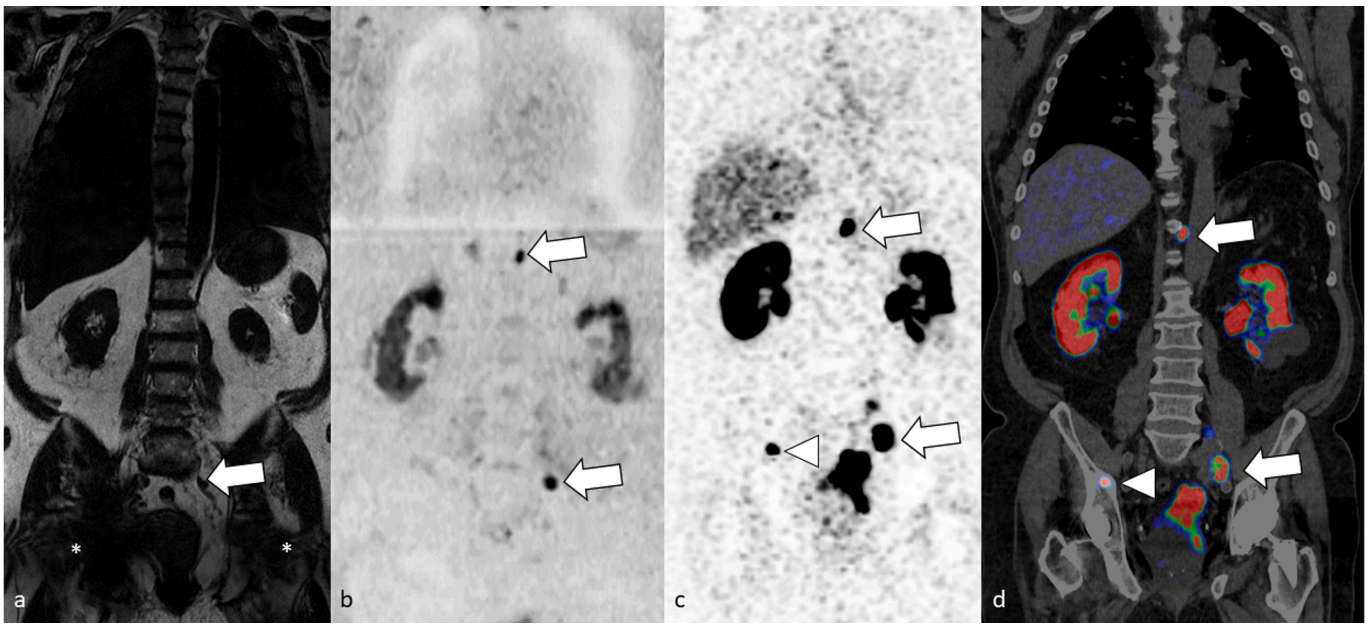

Fig. 8. Discordant distant extension between fast "All-in-One" WB-MRI and ^{68}Ga-PSMA-PET/CT, in a 76-year-old man with high-risk PCa. Coronal WB-MRI T1 Dixon Fat only (a), and coronal reformatted DWIBS (b = 1000 s/mm^2; inverted grayscale) showed vertebral bone lesion and left locoregional lymphnode metastasis (arrow) (b). Bilateral total hip replacement (*) was responsible for artefacts. ^{68}Ga-PSMA-PET/CT (c), and reformatted fused PET/CT showing one more 5 mm bone lesion of the right iliac bone not shown on WB-MRI due to total hip replacement (arrowhead) (c).

1007, with better spatial resolution and lower urinary excretion showed higher detection rate of T3a-T3b [37].

Regarding locoregional metastatic lymph node assessment, PSMA-PET/CT had a superior performance compared to MRI, with an increased detection rate of + 12 % of lesions. This observation is consistent with the results of previous studies and recent *meta*-analysis that compared PSMA and mp-MRI in the staging of newly diagnosed PCa patients [17]. This difference of performance is attributed to the fact that the detection of metastatic lymph nodes on WB-MRI is based solely on the measurement of the smallest axis of the lymph node with a threshold of 8 to 10 mm [38]. In our study, pathological lymph nodes detected by PSMA-PET/CT, which relies only on the PSMA expression and SUV max of the lesion, had a size of 5 mm +/- 1.5 mm, which is below the threshold for positivity on WB-MRI.

Regarding distant staging, both imaging techniques had very similar value in assessing metastatic disease (M1b and M1c). This finding is consistent with our previous publication, which shows no significant difference in distant staging between the two techniques [38]. Semi-quantitative assessment (M1b) showed very good agreement between both techniques, although MRI detected fewer bone metastases, as lesions measuring less than 5 mm did not meet the MET-RADS-P inclusion criteria (10 mm). This discrepancy may affect the overall staging per patient and, in particular, the classification of oligometastatic patients using WB-MRI. However, according to the current literature, this does not affect the clinical management of patients, as there are insufficient randomized clinical trials comparing WB-MRI and PSMA-PET/CT in this new therapeutic area [39,40].

This prospective study has limitations, including its monocentric, retrospective design and small cohort size limiting the statistical power. However, we did not find any previous study in the literature of simultaneous "All-in-One" WB-MRI and PSMA-PET/CT. As previously mentioned, only 8 patients had radical prostatectomy, which did not allow to perform statistical tests to compare T staging and EPE extension as evaluated by both imaging modalities.

Of note, another clinical trial evaluating an "All-in-One" WB-MRI approach is underway with an estimated completion date of August 2026 and a sample size of 400 patients. This new trial will compare the fast "All-in-One" approach to conventional (BS + CT) imaging (ClinicalTrials.gov ID: NCT06071195).

PSMA-PET/CT scans were acquired as routine clinical examination, without an optimized protocol, and read by a nuclear medicine physician. Further trials should aim to compare WB-MRI with optimized PSMA-PET/CT examinations, especially for T staging (for example using a tracer with less urinary excretion, e.g. using 18F-PSMA −1007).

Inter- and intra-reader agreements were not assessed. However, the PSMA-RADS template is known to be highly reproducible [41]. Inter-reader agreement of the Pi-RADS lexicon v.2 has been demonstrated [42]. Excellent inter-reader agreement has also been shown for WB-MRI [43].

Recent and future technological advances will undoubtedly allow further acceleration of MRI examinations for the "All-In-One" staging. For prostate imaging, Bischoff L.M. et al. demonstrated a 36 % decrease in acquisition time for T2 FSE sequences by using deep-learning reconstruction of low resolution T2 FSE sequences rather than standard FSE T2 sequences, while maintaining excellent agreement in Pi-RADS scores [44]. For WB-MRI, the application of a deep-learning based reconstruction significantly improved the signal-to-noise ratio and reduced the acquisition time of DWI sequences by a factor of >2 [45]. Other recent studies showed the increasing impact of deep-learning techniques on MR protocol acceleration [46].

5. Conclusion

A non-irradiating fast "All-In-One" WB-MRI protocol for TNM staging of PCa is feasible in less than 30 min. Compared to PSMA-PET/CT, this protocol offers native superiority for the anatomical (T) assessment, provides a comparable categorical result for distant (M) staging, but detects less nodal metastases.

6. Summary Statement

A fast "All-in-One" WB-MRI is feasible in less than 30 min and offers high diagnostic accuracy for TNM staging of prostate cancer.

Funding for this study

This study was supported by a research grant from GE HealthCare, contract number RA-001834. GE HealthCare provided funding for the project but was not involved in the study design, data collection, analysis, or manuscript preparation. The authors declare no other conflicts of interest related to this study. All opinions and interpretations are solely those of the authors.

CRediT authorship contribution statement

Sandy Van Nieuwenhove: Writing – review & editing, Writing – original draft, Visualization, Validation, Supervision, Methodology, Investigation, Formal analysis, Data curation, Conceptualization. **Renaud Lhommel:** Visualization, Validation, Methodology, Investigation, Formal analysis, Data curation, Conceptualization. **Vassiliki Pasoglou:** Visualization, Validation, Investigation, Formal analysis. **Julien Van Damme:** Writing – review & editing, Writing – original draft, Validation, Investigation, Formal analysis, Data curation. **Nicolas Michoux:** Writing – review & editing, Writing – original draft, Visualization, Validation, Supervision, Software, Project administration, Methodology, Formal analysis, Data curation, Conceptualization. **Perrine Triqueneaux:** Writing – review & editing, Supervision, Software, Resources, Project administration, Investigation, Funding acquisition, Data curation. **Bertrand Tombal:** Writing – review & editing, Validation, Supervision, Methodology, Investigation, Formal analysis, Data curation, Conceptualization. **Frédéric E. Lecouvet:** Writing – original draft, Writing – review & editing, Resources, Supervision, Validation, Conceptualization, Funding acquisition, Investigation, Methodology, Project administration, Formal analysis, Visualization.

Declaration of competing interest

The authors declare the following financial interests/personal relationships which may be considered as potential competing interests: [Sandy Van Nieuwenhove reports financial support was provided by University Hospital Saint-Luc. Sandy Van Nieuwenhove reports a relationship with University Hospital Saint-Luc that includes: employment and funding grants. If there are other authors, they declare that they have no known competing financial interests or personal relationships that could have appeared to influence the work reported in this paper. Bertrand TOMBAL reports a relationship with Amgen Europe GmbH that includes: consulting or advisory, speaking and lecture fees, and travel reimbursement. Bertrand TOMBAL reports a relationship with Astellas Pharma US Inc that includes: consulting or advisory, speaking and lecture fees, and travel reimbursement. Bertrand TOMBAL reports a relationship with Bayer AG that includes: consulting or advisory, funding grants, speaking and lecture fees, and travel reimbursement. Bertrand TOMBAL reports a relationship with Ferring Pharmaceuticals Inc that includes: consulting or advisory. Bertrand TOMBAL reports a relationship with Accord Healthcare Ltd that includes: consulting or advisory and travel reimbursement. Bertrand TOMBAL reports a relationship with Janssen Pharmaceuticals Inc that includes: consulting or advisory, speaking and lecture fees, and travel reimbursement. None If there are other authors, they declare that they have no known competing financial interests or personal relationships that could have appeared to influence the work reported in this paper. Frédéric Lecouvet reports financial support was provided by GE Healthcare that includes speaking and lecture fees and funding grants. Frédéric Lecouvet reports a relationship with University Hospital Saint-Luc that includes: employment If there are other authors, they declare that they have no known competing financial interests or personal relationships that could have appeared to influence the work reported in this paper. Julien Van Damme reports financial support was provided by Astellas, Bristol Myers-Squibb, that includes: speaking and lecture fees. Julien Van Damme reports financial support was provided by Bayer that includes: speaking and lecture fees. Julien Van Damme reports financial support was provided by Bristol Myers-Squibb that includes: speaking and lecture fees. Julien Van Damme reports financial support was provided by Janssens that includes: speaking, scientific advices and lecture fees. Julien Van Damme reports financial support was provided by Sanofi that includes: speaking and lecture fees. Julien Van Damme reports financial support was provided by Ipsen that includes: speaking, scientific advices and lecture fees. Julien Van Damme reports financial support was provided by Sanofi that includes: speaking and lecture fees. Julien Van Damme reports financial support was provided by MSD that includes: speaking, scientific advices and lecture fees. If there are other authors, they declare that they have no known competing financial interests or personal relationships that could have appeared to influence the work reported in this paper. The following authors (Renaud Lhommel, Vassiliki Pasoglou, Nicolas Michoux, Perrine Triqueneaux) declare that they have no known competing financial interests or personal relationships that could have appeared to influence the work reported in this paper].

References

[1] S. Trecarten, A.G. Sunnapwar, G.D. Clarke, M.A. Liss, Prostate MRI for the detection of clinically significant prostate cancer: update and future directions, Adv. Cancer Res. 161 (2024) 71–118, https://doi.org/10.1016/bs.acr.2024.04.002.

[2] M.S. Hofman, N. Lawrentschuk, R.J. Francis, C. Tang, I. Vela, P. Thomas, N. Rutherford, J.M. Martin, M. Frydenberg, R. Shakher, L.M. Wong, K. Taubman, S. Ting Lee, E. Hsiao, P. Roach, M. Nottage, I. Kirkwood, D. Hayne, E. Link, P. Marusic, A. Matera, A. Herschtal, A. Iravani, R.J. Hicks, S. Williams, D. G. Murphy, P.S.G.C. Pro, Prostate-specific membrane antigen PET-CT in patients with high-risk prostate cancer before curative-intent surgery or radiotherapy (proPSMA): a prospective, randomised, multicentre study, Lancet 395 (10231) (2020) 1208–1216, https://doi.org/10.1016/S0140-6736(20)30314-7.

[3] P. Cornford, R.C.N. van den Bergh, E. Briers, T. Van den Broeck, O. Brunckhorst, J. Darraugh, D. Eberli, G. De Meerleer, M. De Santis, A. Farolfi, G. Gandaglia, S. Gillessen, N. Grivas, A.M. Henry, M. Lardas, G. van Leenders, M. Liew, E. Linares Espinos, J. Oldenburg, I.M. van Oort, D.E. Oprea-Lager, G. Ploussard, M.J. Roberts, O. Rouvière, I.G. Schoots, N. Schouten, E.J. Smith, J. Stranne, T. Wiegel, P. M. Willemse, D. Tilki, EAU-EANM-ESTRO-ESUR-ISUP-SIOG Guidelines on Prostate Cancer-2024 update. part i: screening, diagnosis, and local treatment with curative intent, Eur. Urol. 86 (2) (2024) 148–163, https://doi.org/10.1016/j.eururo.2024.03.027.

[4] E. Lopci, G. Lughezzani, V. Fasulo, M. Lazzeri, Re: Stefano Fanti, Alberto Briganti, Louise Emmett, et al. EAU-EANM Consensus Statements on the Role of Prostate-specific Membrane Antigen Positron Emission Tomography/Computed Tomography in Patients with Prostate Cancer and with Respect to [(177)Lu]Lu-PSMA Radioligand Therapy. Eur Urol Oncol. 2022;5:530-6: Extended Use of PSMA PET/CT in Candidates for Focal Therapy, Eur Urol Oncol 5(5) (2022) 601-60210.1016/j.euo.2022.06.006.

[5] E.J. Trabulsi, R.B. Rumble, H. Jadvar, T. Hope, M. Pomper, B. Turkbey, A. B. Rosenkrantz, S. Verma, D.J. Margolis, A. Froemming, A. Oto, A. Purysko, M. I. Milowsky, H.P. Schlemmer, M. Eiber, M.J. Morris, P.L. Choyke, A. Padhani, J. Oldan, S. Fanti, S. Jain, P.A. Pinto, K.A. Keegan, C.R. Porter, J.A. Coleman, G. S. Bauman, A.B. Jani, J.M. Kamradt, W. Sholes, H.A. Vargas, Optimum imaging strategies for advanced prostate cancer: ASCO guideline, J. Clin. Oncol. 38 (17) (2020) 1963–1996, https://doi.org/10.1200/jco.19.02757.

[6] V. Pasoglou, A. Larbi, L. Collette, L. Annet, F. Jamar, J.P. Machiels, N. Michoux, B. C. Vande Berg, B. Tombal, F.E. Lecouvet, One-step TNM staging of high-risk prostate cancer using magnetic resonance imaging (MRI): toward an upfront simplified "all-in-one" imaging approach? Prostate 74 (5) (2014) 469–477, https://doi.org/10.1002/pros.22764.

[7] N.L. Robertson, E. Sala, M. Benz, J. Landa, P. Scardino, H.I. Scher, H. Hricak, H. A. Vargas, Combined whole body and multiparametric prostate magnetic resonance imaging as a 1-step approach to the simultaneous assessment of local recurrence and metastatic disease after radical prostatectomy, J. Urol. 198 (1) (2017) 65–70, https://doi.org/10.1016/j.juro.2017.02.071.

[8] F.E. Lecouvet, V. Pasoglou, S. Van Nieuwenhove, T. Van Haver, Q. de Broqueville, V. Denolin, P. Triqueneaux, B. Tombal, N. Michoux, Shortening the acquisition time of whole-body MRI: 3D T1 gradient echo Dixon vs fast spin echo for metastatic screening in prostate cancer, Eur. Radiol. 30 (6) (2020) 3083–3093, https://doi.org/10.1007/s00330-019-06515-y.

[9] S. Van Nieuwenhove, J. Van Damme, A.R. Padhani, V. Vandecaveye, B. Tombal, J. Wuts, V. Pasoglou, F.E. Lecouvet, Whole-body magnetic resonance imaging for prostate cancer assessment: current status and future directions, J. Magn. Reson Imag. 55 (3) (2022) 653–680, https://doi.org/10.1002/jmri.27485.

[10] B. Turkbey, A.B. Rosenkrantz, M.A. Haider, A.R. Padhani, G. Villeirs, K.J. Macura, C.M. Tempany, P.L. Choyke, F. Cornud, D.J. Margolis, H.C. Thoeny, S. Verma, J. Barentsz, J.C. Weinreb, Prostate Imaging Reporting and Data System Version 2.1: 2019 Update of Prostate Imaging Reporting and Data System Version 2, Eur. Urol. 76 (3) (2019) 340–351, https://doi.org/10.1016/j.eururo.2019.02.033.

[11] M. Abramson, M. DeMasi, D. Zhu, L. Hines, W. Lin, D. Kanmaniraja, V. Chernyak, I. Agalliu, K.L. Watts, Biparametric versus multiparametric MRI for the detection of clinically significant prostate cancer in a diverse, multiethnic population, Abdominal Radiol. (New York) 49 (7) (2024) 2491–2498, https://doi.org/10.1007/s00261-024-04332-6.

[12] N. Schieda, Y. Nisha, A.R. Hadziomerovic, S. Prabhakar, T.A. Flood, R.H. Breau, T. A. McGrath, T. Ramsay, C. Morash, Comparison of positive predictive values of biparametric MRI and multiparametric MRI-directed transrectal US-guided targeted prostate biopsy, Radiology 311 (3) (2024) e231383, https://doi.org/10.1148/radiol.231383.

[13] A. Birosh, E. Salinas-Miranda, R.H. Breau, M.D.F. McInnes, C. Morash, N. Schieda, Multiparametric versus biparametric prostate MRI: comparison of NPV for clinically significant prostate cancer, AJR Am. J. Roentgenol. 222 (3) (2024) e2330496, https://doi.org/10.2214/ajr.23.30496.

[14] E.J. Bass, A. Pantovic, M. Connor, R. Gabe, A.R. Padhani, A. Rockall, H. Sokhi, H. Tam, M. Winkler, H.U. Ahmed, A systematic review and meta-analysis of the diagnostic accuracy of biparametric prostate MRI for prostate cancer in men at risk, Prostate Cancer Prostatic Dis. 24 (3) (2021) 596–611, https://doi.org/10.1038/s41391-020-00298-w.

[15] S. Van Nieuwenhove, T.P. Saussez, S. Thiry, P. Trefois, L. Annet, N. Michoux, F. Lecouvet, B. Tombal, Prospective comparison of a fast 1.5-T biparametric with the 3.0-T multiparametric ESUR magnetic resonance imaging protocol as a triage test for men at risk of prostate cancer, BJU Int. 123 (3) (2019) 411–420, https://doi.org/10.1111/bju.14538.

[16] D. Tilki, R.C.N. van den Bergh, E. Briers, T. Van den Broeck, O. Brunckhorst, J. Darraugh, D. Eberli, G. De Meerleer, M. De Santis, A. Farolfi, G. Gandaglia, S. Gillessen, N. Grivas, A.M. Henry, M. Lardas, J.L.H.v.L.G. Liew, E. Linares Espinos, J. Oldenburg, I.M. van Oort, D.E. Oprea-Lager, G. Ploussard, M.J. Roberts, O. Rouvière, I.G. Schoots, N. Schouten, E.J. Smith, J. Stranne, T. Wiegel, P. M. Willemse, P. Cornford, EAU-EANM-ESTRO-ESUR-ISUP-SIOG guidelines on prostate cancer. part II-2024 update: treatment of relapsing and metastatic prostate cancer, Eur. Urol. 86 (2) (2024) 164–182, https://doi.org/10.1016/j.eururo.2024.04.010.

[17] J. Ma, Q. Yang, X. Ye, W. Xu, Y. Chang, R. Chen, Y. Wang, M. Luo, Y. Lou, X. Yang, D. Li, Y. Xu, W. He, M. Cai, W. Cao, G. Ju, L. Yin, J. Wang, J. Ren, Z. Ma, C. Zuo, S. Ren, Head-to-head comparison of prostate-specific membrane antigen PET and multiparametric MRI in the diagnosis of pretreatment patients with prostate cancer: a meta-analysis, Eur. Radiol. 34 (6) (2024) 4017–4037, https://doi.org/10.1007/s00330-023-10436-2.

[18] S. Jendoubi, M. Wagner, S. Montagne, M. Ezziane, J. Mespoulet, E. Comperat, C. Estellat, A. Baptiste, R. Renard-Penna, MRI for prostate cancer: can computed high b-value DWI replace native acquisitions? Eur. Radiol. 29 (10) (2019) 5197–5204, https://doi.org/10.1007/s00330-019-06085-z.

[19] N. Adubeiro, M.L. Nogueira, R.G. Nunes, H.A. Ferreira, E. Ribeiro, J.M.F. La Fuente, Apparent diffusion coefficient in the analysis of prostate cancer: determination of optimal b-value pair to differentiate normal from malignant tissue, Clin. Imag. 47 (2018) 90–95, https://doi.org/10.1016/j.clinimag.2017.09.004.

[20] A.B. Rosenkrantz, G.L. Bennett, A. Doshi, F.M. Deng, J.S. Babb, S.S. Taneja, T2-weighted imaging of the prostate: Impact of the BLADE technique on image quality and tumor assessment, Abdom. Imag. 40 (3) (2015) 552–559, https://doi.org/10.1007/s00261-014-0225-7.

[21] A.R. Padhani, F.E. Lecouvet, N. Tunariu, D.M. Koh, F. De Keyzer, D.J. Collins, E. Sala, H.P. Schlemmer, G. Petralia, H.A. Vargas, S. Fanti, H.B. Tombal, J. de Bono, METastasis reporting and data system for prostate cancer: practical guidelines for acquisition, interpretation, and reporting of whole-body magnetic resonance imaging-based evaluations of multiorgan involvement in advanced prostate cancer, Eur. Urol. 71 (1) (2017) 81–92, https://doi.org/10.1016/j.eururo.2016.05.033.

[22] S.P. Rowe, K.J. Pienta, M.G. Pomper, M.A. Gorin, Proposal for a Structured Reporting System for Prostate-Specific Membrane Antigen-Targeted PET Imaging: PSMA-RADS Version 1.0, Journal of nuclear medicine: official publication, Society of Nuclear Medicine 59(3) (2018) 479-48510.2967/jnumed.117.195255.

[23] S. Mehralivand, J.H. Shih, S. Harmon, C. Smith, J. Bloom, M. Czarniecki, S. Gold, G. Hale, K. Rayn, M.J. Merino, B.J. Wood, P.A. Pinto, P.L. Choyke, B. Turkbey, A grading system for the assessment of risk of extraprostatic extension of prostate cancer at multiparametric MRI, Radiology 290 (3) (2019) 709–719, https://doi.org/10.1148/radiol.2018181278.

[24] T. Ucar, N. Gunduz, E. Demirci, M. Culpan, H. Gunel, G. Kir, R.G. Atis, A. Yildirim, Comparison of 68Ga-PSMA PET/CT and mp-MRI in regard to local staging for prostate cancer with histopathological results: a retrospective study, Prostate 82 (15) (2022) 1462–1468, https://doi.org/10.1002/pros.24420.

[25] S.P. Rowe, K.J. Pienta, M.G. Pomper, M.A. Gorin, PSMA-RADS Version 1.0: A step towards standardizing the interpretation and reporting of PSMA-targeted PET imaging studies, Eur. Urol. 73 (4) (2018) 485–487, https://doi.org/10.1016/j.eururo.2017.10.027.

[26] K.L. Gwet, Computing inter-rater reliability and its variance in the presence of high agreement, Br. J. Math. Stat. Psychol. 61 (Pt 1) (2008) 29–48, https://doi.org/10.1348/000711006x126600.

[27] S.A. Taylor, S. Mallett, A. Miles, S. Morris, L. Quinn, C.S. Clarke, S. Beare, J. Bridgewater, V. Goh, S. Janes, D.M. Koh, A. Morton, N. Navani, A. Oliver, A. Padhani, S. Punwani, A. Rockall, S. Halligan, Whole-body MRI compared with standard pathways for staging metastatic disease in lung and colorectal cancer: the Streamline diagnostic accuracy studies, Health Technol. Assess. (Winchester, England) 23 (66) (2019) 1–270, https://doi.org/10.3310/hta23660.

[28] Y. Wang, J.R. Galante, A. Haroon, S. Wan, A. Afaq, H. Payne, J. Bomanji, S. Adeleke, V. Kasivisvanathan, The future of PSMA PET and WB MRI as next-generation imaging tools in prostate cancer, Nat. Rev. Urol. 19 (8) (2022) 475–493, https://doi.org/10.1038/s41585-022-00618-w.

[29] F.E. Lecouvet, D.E. Oprea-Lager, Y. Liu, P. Ost, L. Bidaut, L. Collette, C.M. Deroose, K. Goffin, K. Herrmann, O.S. Hoekstra, G. Kramer, Y. Lievens, E. Lopci, D. Pasquier, L.J. Petersen, J.N. Talbot, H. Zacho, B. Tombal, N.M. deSouza, Use of modern imaging methods to facilitate trials of metastasis-directed therapy for oligometastatic disease in prostate cancer: a consensus recommendation from the EORTC Imaging Group, Lancet Oncol. 19 (10) (2018) e534–e545, https://doi.org/10.1016/S1470-2045(18)30571-0.

[30] J. Morote, A. Celma, S. Roche, I.M. de Torres, R. Mast, M.E. Semedey, L. Regis, J. Planas, Who benefits from multiparametric magnetic resonance imaging after suspicion of prostate cancer? Eur. Urol. Oncol. 2 (6) (2019) 664–669, https://doi.org/10.1016/j.euo.2018.11.009.

[31] L. Emmett, J. Buteau, N. Papa, D. Moon, J. Thompson, M.J. Roberts, K. Rasiah, D. A. Pattison, J. Yaxley, P. Thomas, A.C. Hutton, S. Agrawal, A. Amin, A. Blazevski, V. Chalasani, B. Ho, A. Nguyen, V. Liu, J. Lee, G. Sheehan-Dare, R. Kooner, G. Coughlin, L. Chan, T. Cusick, B. Namdarian, J. Kapoor, O. Alghazo, H.H. Woo, N. Lawrentschuk, D. Murphy, M.S. Hofman, P. Stricker, The additive diagnostic value of prostate-specific membrane antigen positron emission tomography computed tomography to multiparametric magnetic resonance imaging triage in the diagnosis of prostate cancer (PRIMARY): a prospective multicentre study, Eur. Urol. 80 (6) (2021) 682–689, https://doi.org/10.1016/j.eururo.2021.08.002.

[32] M. Thalgott, C. Düwel, I. Rauscher, M.M. Heck, B. Haller, A. Gafita, J.E. Gschwend, M. Schwaiger, T. Maurer, M. Eiber, One-stop-shop whole-body (68)Ga-PSMA-11 PET/MRI compared with clinical nomograms for preoperative T and N staging of high-risk prostate cancer, J. Nucl. Med.: Offi. Publ., Soc. Nucl. Med. 59 (12) (2018) 1850–1856, https://doi.org/10.2967/jnumed.117.207696.

[33] X. Ren, M. Nur Salihin Yusoff, N. Hartini Mohd Taib, L. Zhang, K. Wang, (68)Ga-prostate specific membrane antigen-11 PET/CT versus multiparametric MRI in the detection of primary prostate cancer: a systematic review and head-to-head comparative meta-analysis, Eur. J. Radiol. 170 (2024) 111274, https://doi.org/10.1016/j.ejrad.2023.111274.

[34] A. Iravani, M.S. Hofman, T. Mulcahy, S. Williams, D. Murphy, B.K. Parameswaran, R.J. Hicks, (68)Ga PSMA-11 PET with CT urography protocol in the initial staging and biochemical relapse of prostate cancer, Cancer Imag. 17 (1) (2017) 31, https://doi.org/10.1186/s40644-017-0133-5.

[35] A. Arslan, E. Karaarslan, A.L. Güner, Y. Sağlıcan, M.B. Tuna, O. Özışık, A.R. Kural, Comparison of MRI PSMA PET/CT, and fusion PSMA PET/MRI for detection of clinically significant prostate cancer, J. Comput. Assist. Tomogr. 45 (2) (2021) 210–217, https://doi.org/10.1097/rct.0000000000001116.

[36] C.J. von Klot, A.S. Merseburger, A. Böker, S. Schmuck, T.L. Ross, F.M. Bengel, M. A. Kuczyk, C. Henkenberens, H. Christiansen, H.J. Wester, W. Solass, M. Lafos, T. Derlin, (68)Ga-PSMA PET/CT imaging predicting intraprostatic tumor extent extracapsular extension and seminal vesicle invasion prior to radical prostatectomy in patients with prostate cancer, Nucl. Med. Mol. Imag. 51 (4) (2017) 314–322, https://doi.org/10.1007/s13139-017-0476-7.

[37] B.S. Abrahamsen, T. Tandstad, B.Y. Aksnessæther, T.V. Bogsrud, M. Castillejo, E. Hernes, H. Johansen, T.M.I. Keil, I.S. Knudtsen, S. Langørgen, K.M. Selnæs, T. F. Bathen, M. Elschot, Added value of [18F]PSMA-1007 PET/CT and PET/MRI in patients with biochemically recurrent prostate cancer: impact on detection rates and clinical management, J. Magn. Reson. Imag. (2024), https://doi.org/10.1002/jmri.29386.

[38] J. Van Damme, B. Tombal, L. Collette, S. Van Nieuwenhove, V. Pasoglou, T. Gerard, F. Jamar, R. Lhommel, F.E. Lecouvet, Comparison of (68)Ga-prostate specific membrane antigen (PSMA) positron emission tomography computed tomography (PET-CT) and whole-body magnetic resonance imaging (WB-MRI) with diffusion sequences (DWI) in the staging of advanced prostate cancer, Cancers (Basel) 13 (21) (2021), https://doi.org/10.3390/cancers13215286.

[39] B. Bernard, B. Gershman, R.J. Karnes, C.J. Sweeney, N. Vapiwala, Approach to oligometastatic prostate cancer, Am. Soc. Clin. Oncol. Educ. Book 35 (2016) 119–129, https://doi.org/10.1200/edbk_159241.

[40] A. Farolfi, B. Hadaschik, F.C. Hamdy, K. Herrmann, M.S. Hofman, D.G. Murphy, P. Ost, A.R. Padhani, S. Fanti, Positron emission tomography and whole-body magnetic resonance imaging for metastasis-directed therapy in hormone-sensitive oligometastatic prostate cancer after primary radical treatment: a systematic review, Eur. Urol. Oncol. 4 (5) (2021) 714–730, https://doi.org/10.1016/j.euo.2021.02.003.

[41] E. Demirci, R. Akyel, B. Caner, N. Alan-Selçuk, Ş. Güven-Meşe, M. Ocak, L. Kabasakal, Interobserver and intraobserver agreement on prostate-specific membrane antigen PET/CT images according to the miTNM and PSMA-RADS criteria, Nucl. Med. Commun. 41 (8) (2020) 759–767, https://doi.org/10.1097/mnm.0000000000001219.

[42] A.B. Rosenkrantz, L.A. Ginocchio, D. Cornfeld, A.T. Froemming, R.T. Gupta, B. Turkbey, A.C. Westphalen, J.S. Babb, D.J. Margolis, Interobserver reproducibility of the PI-RADS version 2 lexicon: a multicenter study of six experienced prostate radiologists, Radiology 280 (3) (2016) 793–804, https://doi.org/10.1148/radiol.2016152542.

[43] P. Pricolo, E. Ancona, P. Summers, J. Abreu-Gomez, S. Alessi, B.A. Jereczek-Fossa, O. De Cobelli, F. Nole, G. Renne, M. Bellomi, A.R. Padhani, G. Petralia, Whole-body magnetic resonance imaging (WB-MRI) reporting with the METastasis Reporting and Data System for Prostate Cancer (MET-RADS-P): inter-observer agreement between readers of different expertise levels, Cancer Imag. 20 (1) (2020), https://doi.org/10.1186/s40644-020-00350-x.

[44] L.M. Bischoff, J.M. Peeters, L. Weinhold, P. Krausewitz, J. Ellinger, C. Katemann, A. Isaak, O.M. Weber, D. Kuetting, U. Attenberger, C.C. Pieper, A.M. Sprinkart, J. A. Luetkens, Deep learning super-resolution reconstruction for fast and motion-robust T2-weighted Prostate MRI, Radiology 308 (3) (2023) e230427, https://doi.org/10.1148/radiol.230427.

[45] A. Ponsiglione, W. McGuire, G. Petralia, M. Fennessy, T. Benkert, A.M. Ponsiglione, A.R. Padhani, Image quality of whole-body diffusion MR images comparing deep-learning accelerated and conventional sequences, Eur. Radiol. 34 (12) (2024) 7985–7993, https://doi.org/10.1007/s00330-024-10883-5.

[46] M. Safari, Z. Eidex, C.W. Chang, R.L.J. Qiu, X. Yang, Fast MRI reconstruction using deep learning-based compressed sensing: a systematic review, ArXiv (2024).